

Multiple injections of pegylated liposomal doxorubicin: pharmacokinetics and therapeutic activity. *

Gregory J.R. Charrois and Theresa M. Allen

Department of Pharmacology

University of Alberta

Edmonton, Alberta

Canada

T6G 2H7

Running title: Multiple injections of pegylated liposomal doxorubicin

Corresponding author: Theresa M. Allen

Phone: (780) 492-5710

Fax: (780) 492-8078

email: terry.allen@ualberta.ca

Number of text pages: 45 including figures and tables

Number of tables: 3

Number of figures: 6

Number of references: 39

Number of words in:

Abstract: 249

Introduction: 708

Discussion: 1500

Abbreviations:

SL-DXR, pegylated (STEALTH[®]) liposomal doxorubicin (Doxil[®]/Caelyx[®]); PPE, palmar-plantar erythrodysesthesia; D5W, dextrose 5% in sterile water; MEM, minimal essential media; AUC, area under the plasma/tissue concentration versus time curve; $t_{1/2}$, tissue clearance half-life; C_{ss} , steady state concentration; C_{max} , maximal tissue drug concentration; MPS, mononuclear phagocyte system

Recommended section: Absorption, Distribution, Metabolism & Excretion OR
Chemotherapy, Antibiotics, & Gene Therapy

ABSTRACT

Effects of multiple injections of liposomal doxorubicin on pharmacokinetics, therapeutic outcome, and toxicity were studied in mice using different dosing schedules and dose intensities. Biodistribution of doxorubicin to the cutaneous tissues of mice (skin and paws) and to orthotopically implanted mammary tumors (4T1) was examined. Weekly intravenous administration of pegylated (STEALTH[®]) liposomal doxorubicin (SL-DXR) at a dose of 9 mg/kg (q1wk x 4 doses) resulted in accumulation of doxorubicin in cutaneous tissues of mice, and development of lesions resembling palmar-plantar erythrodysesthesia (PPE). Lengthening the dose interval to q2wk x 4 reduced the accumulation of doxorubicin and lowered the incidence of PPE-like lesions. A dose interval of q4wk x 4 resulted in complete clearance of doxorubicin from tissues between subsequent doses and a negligible incidence of PPE-like lesions. Doses of 9 mg/kg SL-DXR given at q1wk x 2 or q2wk x 2 had similar therapeutic activities, while prolonging the dose interval to q4wk x 2 reduced therapeutic activity. Pharmacokinetics, biodistribution, and therapeutic activity were studied in tumor-bearing mice for three dose schedules having the same dose intensity (4.5 mg/kg q3d x 4, 9 mg/kg q1wk x 2, or 18 mg/kg q2wk x 1). For these schedules, larger doses administered less often tended to be superior therapeutically to smaller doses given more often. These data provide the first pharmacokinetic measurements of doxorubicin concentrations in cutaneous tissues and tumors with repeat administration of liposomal formulations, and they provide a useful model for the study of factors leading to PPE in humans.

Pegylated (STEALTH[®]) liposomal doxorubicin (Doxil[®]/Caelyx[®]) (SL-DXR) is a long-circulating formulation of liposomal doxorubicin that is currently approved for use in AIDS-related Kaposi's sarcoma and refractory ovarian cancer. It has also shown activity in other tumors, including metastatic breast cancer (Northfelt et al., 1997; Ranson et al., 1997; Gordon et al., 2000). As reviewed by Allen et al., STEALTH[®] liposomes have dose-independent, log-linear pharmacokinetics (Allen et al., 1995). Encapsulating doxorubicin within these liposomes alters its pharmacokinetics and biodistribution and results in a decrease in doxorubicin-associated toxicities, including its dose-limiting cardiomyopathy and myelosuppression (Berry et al., 1998; Safra et al., 2000). The dose-limiting toxicities of SL-DXR are mucocutaneous reactions such as palmar-plantar erythrodysesthesia (PPE) and mucositis/stomatitis (Gordon et al., 1995; Uziely et al., 1995; Lotem et al., 2000; Hamilton et al., 2002).

Palmar-plantar erythrodysesthesia primarily affects the palms of the hands and the soles of the feet. Patients who develop PPE experience erythema and edema that can lead to blistering desquamation if the next dose is not delayed or reduced. The current hypothesis for the development of PPE is that the small size (100 nm diameter) and long circulation time ($t_{1/2}$ is approximately 48 hours in humans) of SL-DXR allows liposomes to accumulate in the skin. The basal layers of the skin are damaged with prolonged exposure to doxorubicin as the liposomes slowly release their contents. The accumulation of liposomes is thought to mimic the anatomical distribution of lesions and to be greatest in regions of skin that are subjected to pressure or irritation, such as the flexure creases of the hands, soles of the feet, or belt lines (Gordon et al., 1995; Lotem et al., 2000).

This hypothesis is supported by current experimental and clinical data. Liposomes with long circulation times accumulate in the skin of experimental animals to a greater extent than liposomes with shorter circulation times (Allen et al., 1991; Papahadjopoulos et al., 1991). In mice, this accumulation is dependent on liposome size; further, mouse paws (homologous to human hands and feet) accumulate more liposomes than skin, supporting the idea of the pressure-dependent extravasation of liposomes into cutaneous tissues (Charrois and Allen, 2003). This hypothesis is further supported by the observation that Myocet™, another liposome formulation of doxorubicin, does not produce PPE and has myelosuppression as its dose-limiting toxicity. Myocet differs from Doxil® in having a larger mean diameter (160 nm vs. 100 nm), a shorter plasma $t_{1/2}$ (6.7 hours vs. 45.2 hours), and a larger volume of distribution (18.8 L vs. 4 L) (Cowens et al., 1993; Gabizon et al., 1994a).

Clinical data suggest that PPE is more likely to develop after multiple doses of SL-DXR. In addition, the likelihood of developing PPE is related to the dose intensity of SL-DXR therapy, with patients receiving greater than 10 to 12 mg/m²/week more likely to develop symptoms (Gabizon et al., 1994b; Muggia et al., 1997; Ranson et al., 1997). When PPE develops, clinical interventions include lengthening the dose interval and/or decreasing the dose intensity. However, either of these interventions may compromise the therapeutic outcome (Hensley et al., 2001).

Despite the widespread clinical use of SL-DXR, few studies have looked at the pharmacokinetics and biodistribution of repeat injections in experimental models, and no studies have quantified the cutaneous localization of doxorubicin from SL-DXR with repeat administration (Amantea et al., 1999). Therefore, a small-animal model for the

pharmacokinetics and biodistribution of doxorubicin (from SL-DXR) in plasma, tumor, and cutaneous tissues will be beneficial in understanding the relationship between the dose schedule and dose intensity of SL-DXR therapy and its therapeutic activity and toxicity. We performed experiments studying the plasma pharmacokinetics and biodistribution of doxorubicin to the skin and paws of mice as a function of time using either the same dose of SL-DXR and different dose intervals (i.e., different dose intensities), or different dose schedules with the same dose intensity. The latter experiments included tumor tissue (4T1 murine mammary carcinoma) and were performed to test the hypothesis that, for a given dose intensity, it is therapeutically beneficial to administer larger infrequent doses than smaller more frequent doses (Gabizon, 2001). Therapeutic experiments were also performed using the 4T1 murine mammary carcinoma model to determine if altering either the dose schedule or the dose intensity affects the therapeutic activity of SL-DXR.

METHODS

Chemicals and Reagents

SL-DXR (STEALTH[®] liposomal doxorubicin, Doxil[®]/Caelyx[®]) was a generous gift from ALZA Corporation (Mountain View, CA). Dextrose USP (D5W), 5% wt/vol in water (Baxter Toronto, ON, Canada), was purchased from the pharmacy at the University of Alberta Hospitals. Minimal essential medium (MEM) was from Sigma Chemical Co. (St. Louis, MO). Fetal bovine serum, penicillin, and streptomycin were from Life Technologies, Inc. (Burlington, ON, Canada). All other chemicals were of the highest grade available.

Animals and Tumor Model

Female BALB/c mice (6-8 weeks) were purchased from the breeding colony at the Health Sciences Laboratory Animal Services, University of Alberta. Mice were housed under standard conditions and had access to food and water *ad libitum*. All animal protocols were approved by the Health Sciences Animal Policy and Welfare Committee, University of Alberta, and are in accordance with the Guide to the Care and Use of Experimental Animals set forth by the Canadian Council on Animal Care.

Pharmacokinetics and Biodistribution

Pharmacokinetic and biodistribution studies were carried out in either tumor-free mice or in mice bearing murine mammary carcinoma (see below). The SL-DXR was diluted in D5W, and 200 μ L was injected intravenously (i.v.) via the lateral tail vein. In tumor-free mice, 4 doses of 9 mg/kg (27 mg/m²) SL-DXR were administered either weekly (q1wk x 4), every 2 weeks (q2wk x 4), or every 4 weeks (q4wk x 4) for a total dose of 36 mg/kg. The dose intensities for these schedules were 9 mg/kg/wk (27

mg/m²/wk), 4.5 mg/kg/wk (13.5 mg/m²/wk), and 2.25 mg/kg/wk (6.75 mg/m²/wk), respectively (Freireich et al., 1966). In experiments at the same dose intensity, tumor-bearing mice received 9 mg/kg/wk (27 mg/m²/wk) of SL-DXR using either 4 doses of 4.5 mg/kg (q3d), 2 doses of 9 mg/kg (q1wk), or 1 dose of 18 mg/kg (q2wk). At various time points after each injection, mice were euthanized (n=4-5), blood was collected with a heparinized syringe, and plasma was isolated by centrifugation (3000g for 5 minutes). Organs were removed and doxorubicin quantified as described below.

Pharmacokinetic parameters were calculated for total doxorubicin. The area under the concentration versus time curve (AUC) was calculated using the trapezoidal rule. Plasma half-lives ($t_{1/2}$) were calculated using the formula $t_{1/2}=0.693/k_{elm}$, where k_{elm} is the elimination constant derived from the plasma concentration versus time curve. Tissue $t_{1/2}$ was calculated in a similar manner, using the terminal slope of the tissue concentration versus time curve; $t_{1/2}$ was not calculated for q3d or q1wk dosing, as there were not sufficient time points in the terminal portion of the curves. For experiments using different dose intensities, the average steady state concentration (C_{ss}) was calculated by taking the fourth dose AUC (taken as steady state) as determined by the trapezoidal rule and dividing by the dose interval in hours.

Quantification of Doxorubicin

Total tissue doxorubicin was quantified using a method similar to that of Mayer et al. (Mayer et al., 1997). Briefly, tissue homogenates of 10% wt/vol were prepared in water. Skin and paws were frozen in liquid nitrogen and crushed with a mortar and pestle before homogenization with a Polytron homogenizer (Brinkmann Instruments, Inc., Mississauga, ON, Canada). Homogenates or 25% plasma (200 μ L) were placed in a 2

mL micro-centrifuge tube, and 100 μ L of 10% (vol/vol) Triton X-100, 200 μ L of water, and 1500 μ L acidified isopropanol (0.75N HCl) were added. The tubes were mixed thoroughly, and the doxorubicin and doxorubicin metabolites (if any) were extracted overnight at -25°C . The next day, the tubes were warmed to room temperature, vortexed for 5 minutes, centrifuged at 15,000g for 20 minutes, and stored at -80°C until analysis. Doxorubicin was quantified fluorometrically ($\lambda_{\text{excitation}}$ 470 nm and $\lambda_{\text{emission}}$ 590 nm). To correct for nonspecific background fluorescence, the samples were analyzed using a standard curve containing tissue extracts derived from drug-free mice. The data represent the mean \pm S.D. of triplicate aliquots from 4 to 5 mice and are expressed as doxorubicin μ equivalents per milliliter of plasma or per gram of tissue, as this assay does not discriminate between doxorubicin and any fluorescent metabolites that may have similar excitation and emission profiles.

Tumor Implantation / Therapeutic Experiments

The 4T1 murine mammary carcinoma was a generous gift from Dr. Fred Miller (Barbara Ann Karmanos Cancer Institute, Detroit, MI) and was maintained in MEM supplemented with 10% fetal bovine serum, penicillin (100 units/mL), and streptomycin (100 μ g/mL) at 37°C in a humidified incubator with a 5% CO_2 atmosphere (Aslakson and Miller, 1992). Tumors were orthotopically implanted as previously described (Moase et al., 2001). Briefly, a small incision was made in the lower abdomen of anaesthetized mice, and 10^5 4T1 cells in 10 μ L supplemented media were implanted in the right No. 4 mammary fat pad. The incision was closed with a surgical wound clip, which was removed 1 week later. For tissue distribution studies in tumor-bearing mice, mice were

injected with the chosen dose of SL-DXR 10 days after tumor implantation, when tumors were large enough to excise. Studies were then performed as described above.

For therapeutic experiments, mice were treated 4 days after tumor implantation. Mice treated with different dose intensities received 9 mg/kg SL-DXR either q1wk x 2, q2wk x 2, or q4wk x 2. When the dose intensity was kept constant, mice received one dose of 18 mg/kg (54 mg/m²), 9 mg/kg (27 mg/m²) q1wk, or 4.5 mg/kg (13.5 mg/m²) q3days for a total drug dose of 18 mg/kg. Tumor growth was monitored by measuring tumor diameters with calipers, and tumor volume was calculated using the formula $v=0.4ab^2$, where a and b represent perpendicular diameters and $a>b$. The experiment was repeated once, and the data represent the mean \pm S.D. from 5 to 10 mice except for the group receiving 18 mg/kg, where $n=4$ to 5 (see Toxicity).

Statistical Analysis

Statistical comparisons were performed using a one-way ANOVA with a Tukey-Kramer post test or Student t-test (as appropriate) with Graph Pad InStat Version 3.01 for Windows 95/NT (GraphPad Software, San Diego CA).

RESULTS

Pharmacokinetics for Different Dose Schedules

Figure 1 presents the plasma, skin, and paw doxorubicin profiles for mice receiving weekly i.v. doses of 9 mg/kg (27 mg/m², q1wk x 4). Results shown in Figure 1A indicate that the drug was not completely cleared from the plasma before administration of subsequent doses. Plasma $t_{1/2}$ values were on the order of 40 hours, and plasma concentrations for each dose peaked at approximately the same values. Plasma AUC values plateaued after the second dose, suggesting that steady state was reached (Table 1).

Skin and paw drug concentrations for a dose schedule of q1wk x 4 are seen in Figures 1B and 1C, respectively. Similar to plasma, doxorubicin was not completely cleared from either tissue between doses. For the first 3 doses of SL-DXR, skin C_{max} was reached 72 hours post-injection ($p < 0.001-0.05$) and at 24 hours after injection for the fourth dose. The nadir occurred at increasing drug levels with each subsequent dose. Skin AUCs increased 3-fold between the first and third doses and then appeared to reach steady state (Table 1).

The C_{max} for total doxorubicin was reached in paws 72 hours after the first dose, but was earlier for subsequent doses ($p < 0.01-0.001$). Paws achieved higher drug concentrations than skin for the first two doses, as reflected in their higher AUC levels, but were similar to skin for the next two doses (Figure 1, Table 1). The nadir drug levels for paws remained high throughout the study and paw levels appeared to reach steady state after the first dose (the AUCs for paws did not change with subsequent doses). The

higher drug levels in paws than in skin may be due to the pressure-dependent extravasation of liposomes as the mice walk around the cage, groom, feed, etc.

Doxorubicin levels in plasma, skin, and paws of mice receiving i.v. SL-DXR at a dose of 9 mg/kg q2wk are presented in Figure 2. Extending the dose interval allowed plasma drug levels to fall to below detectable limits before the next dose of SL-DXR was given. As with the q1wk dosing schedule, plasma AUC values plateaued after the second dose (Table 1).

Skin and paws reached C_{\max} for total doxorubicin for the q2wk x 3 schedule at approximately 72 hours post-injection. Prolonging the dose interval allowed more drug to be cleared from the skin and paws, and the nadir drug levels were significantly lower than those reached for the q1wk dose schedule ($p < 0.001$ for skin and $p < 0.01-0.001$ for paws). Again, paw concentrations of doxorubicin were initially higher than those in skin. However, with subsequent doses, the skin C_{\max} increased ($p < 0.05$ for Dose 1 vs. Doses 3 and 4) while, unexpectedly, the paw C_{\max} decreased significantly between the first and second doses ($p < 0.05$) and between the second and third doses ($p < 0.01$) (Table 1). These changes are also reflected in their respective AUC values (Table 1).

Figure 3 presents results for an i.v. dose schedule of 9 mg/kg SL-DXR q4wk x 4. Peak plasma levels were the same as for the previous two dosing schedules and, as was seen in mice receiving the q2wk x 4 dosing schedule, the longer dose interval resulted in plasma doxorubicin concentrations that were below detectable limits between doses. The $t_{1/2}$ and AUC values were also similar to those for previous dosing schedules (Table 1).

Skin and paw doxorubicin concentrations for this dose schedule are presented in Figures 3B and 3C, respectively. Again, the C_{\max} for total doxorubicin was achieved at

approximately 72 hours post-injection. For this dose schedule, the drug concentrations in both skin and paws fell to low levels before each successive injection. Skin C_{\max} and AUC values increased with each dose (C_{\max} , Dose 1 vs. Dose 4, $p < 0.05$), while those for paws decreased, particularly between the first and subsequent doses (C_{\max} , $p < 0.001$ Dose 1 vs. Dose 2) (Table 1).

The skin and paw clearance $t_{1/2}$ values for doxorubicin are given in Table 1. Skin and paw $t_{1/2}$ values could not be calculated for the q1wk dosing schedule. Modest increases in plasma $t_{1/2}$ were observed for all dosing schedules from the first to fourth dose. Mice receiving 9 mg/kg q2wk or q4wk had greatly increased clearance $t_{1/2}$ values for skin from the first to fourth dose. Mice receiving SL-DXR with a q4wk schedule had an increase in clearance $t_{1/2}$ for paws, while skin $t_{1/2}$ did not change appreciably. The average steady state drug concentration (C_{ss}) for each dose schedule was calculated by dividing the AUC_{ss} (4th dose) by the dose interval in hours (Table 1). As expected, doubling the dose interval resulted in a halving of the C_{ss} values for all tissues.

Toxicity

PPE-like lesions were more frequent in mice receiving the 9 mg/kg q1wk x 4 dose schedule (Table 2). The lesions included hair loss on the mouse's muzzle (area exposed to pressure while the mouse feeds) and red inflamed paws with mild swelling. (The presence of lesions did not, however, have an important effect on the weight of the paws, data not shown). This is consistent with current clinical and laboratory data demonstrating that PPE is more likely to occur with higher Doxil[®] dose intensities (Ranson et al., 1997; Amantea et al., 1999; Lotem et al., 2000).

During these experiments some additional drug toxicity was observed, particularly for the weekly dose schedule. Four mice from the 9 mg/kg q1wk schedule were euthanized due to severe weight loss (3 mice, no cause determined; 1 mouse, heart failure). Three mice from the 9 mg/kg q2wk schedule were euthanized (2 mice, no cause determined; 1 mouse, mild subacute cardiac and hepatic degeneration). In the 9 mg/kg q4wk group, 1 mouse was euthanized due to severe weight loss (no cause determined). The staff veterinary pathologist at the University of Alberta's Health Sciences Laboratory Animal Services performed all postmortem exams.

The total cumulative SL-DXR dose for these animals was high (36 mg/kg, 108 mg/m²). Since toxicity was encountered, mice in the therapeutic experiments received only 2 doses of SL-DXR (18 mg/kg, 54 mg/m² total drug).

Pharmacokinetics for the Same Dose Intensity

To determine the effect of different dose schedules at the same dose intensity, we performed pharmacokinetic and biodistribution experiments in mice bearing the 4T1 murine mammary carcinoma and measured doxorubicin levels in plasma, tumor, skin, and paws. At 10 days post-implantation, when the tumors were well developed, mice were injected i.v. with a total dose of 18 mg/kg SL-DXR (54 mg/m²) given as either 4.5 mg/kg q3d, 9 mg/kg q1wk x 2, or 18 mg/kg q2wk x 1. Tissue concentrations and pharmacokinetic parameters are given in Figure 4 and Table 3.

The results for plasma doxorubicin concentrations are presented in Figure 4A. For mice receiving 4.5 mg/kg q3d, there was a significant increase in plasma C_{max} from the first dose to the second and subsequent doses (p<0.001). In addition, plasma levels appeared to reach steady state after the second dose, as evidenced by the AUCs (Table 3).

As with naïve mice, in tumor-bearing mice receiving 9 mg/kg q1wk there was detectable drug in the plasma at 7 days after injection (Figure 1A vs. Figure 4A). Interestingly, the plasma $t_{1/2}$ and AUC values were lower in tumor-bearing mice than for naïve mice receiving 9 mg/kg q1wk (Table 3 vs. Table 1A). Distribution to the tumor may account for the lower $t_{1/2}$ and tissue AUC values, which is consistent with results from studies using the C26 colon carcinoma tumor model in BALB/c mice (Hong et al., 1999).

A single dose of 18 mg/kg resulted in a plasma C_{max} approximately twice that of the first dose of the 9 mg/kg dose schedule, and approximately 4 times that of the first dose of the 4.5 mg/kg dose schedules (Table 3). For each schedule there is also a linear relationship between the AUC of the first injection and the dose ($r^2=0.9937$). These observations are in line with the dose independence of the plasma pharmacokinetics for single doses of SL-DXR in this dose range (Allen and Hansen, 1991; Gabizon et al., 1994b).

Tumor levels of doxorubicin are given in Figure 4B. For mice receiving 18 mg/kg, and for the first dose at the 4.5 or 9 mg/kg dose schedules, tumor doxorubicin reached C_{max} at 24 hours, which was earlier than skin and paw levels reached C_{max} for the two higher doses. The C_{max} for the dose schedule was approximately double that of the 9 mg/kg q1wk dose schedule and approximately 4-fold higher than the C_{max} for the 4.5 mg/kg q3d dose schedule (Figure 4B), i.e., the C_{max} increased proportionately with dose. The tumor $AUC_{(0-\infty)}$ values were similar for all dose schedules (Table 3).

Skin drug levels from each of the dose schedules are seen in Figure 4C. Results for mice receiving 9 mg/kg were similar to those for non-tumor-bearing mice in that the C_{max} for skin doxorubicin in tumor-bearing mice peaked at 72 hours post-injection. In

addition, the C_{\max} and AUCs for the second dose were higher than the first ($p < 0.0008$, t -test) (Table 1A vs. Table 3, Figure 1B vs. Figure 4C). As with tumor, the doxorubicin C_{\max} in skin increased proportionately with dose (Figure 4C). The total AUC_(0-∞) values for the 18 mg/kg and 9 mg/kg dose schedules were similar, and higher than that seen for the 4.5 mg/kg dose schedule (Table 3). These results demonstrated that skin, like tumor, was exposed to sustained levels of doxorubicin for all three dose schedules, although the 9 and 18 mg/kg schedules resulted in exposure to higher drug concentrations.

As in naïve mice, the paw concentrations of doxorubicin were higher than skin concentrations in tumor-bearing mice, (Figure 4D vs. Figure 1C). For mice receiving 4.5 mg/kg (Figure 4D), the C_{\max} in paws continued to increase for 7 days after initiation of therapy. The C_{\max} in paws also increased proportionately with dose. The AUC_(0-∞) for the 18 mg/kg dose was higher than that for the 9 mg/kg x 2 dose schedule, which in turn was higher than the AUC for the 4.5 mg/kg x 4 dose schedule (Table 3). The increased paw AUC at higher doses may indicate a greater likelihood of developing skin toxicities such as PPE at these doses. For mice receiving 18 mg/kg, the tumor, skin, and paw clearance $t_{1/2}$ values were 117, 90, and 110 hours, respectively. It is notable that the tissue $t_{1/2}$ values were considerably higher than those for plasma $t_{1/2}$ (Table 3). The values for skin and paws are consistent with results from naïve mice receiving SL-DXR with different dose schedules.

Therapeutic Experiments

The results of therapeutic experiments in tumor-bearing mice receiving 9 mg/kg q1wk, q2wk, or q4wk by the i.v. route are presented in Figure 5. Tumor volume can be difficult to measure when tumors exceed 400 mm³; however, tumor growth in control

mice receiving sterile D5W was similar for all dose schedules. The therapeutic activities of SL-DXR were equivalent for mice receiving the drug for either a q1wk x 2 or a q2wk x 2 dose schedule. SL-DXR administered using a q4wk x 2 dose schedule appeared to have reduced therapeutic activity compared to the other two dose regimes. In other words, if the dose interval was too long, antitumor activity was affected adversely. This may have therapeutic implications, as clinical interventions for PPE include lengthening the dose interval or reducing the dose (i.e. reducing the dose intensity) to decrease the incidence and/or severity of PPE.

The results for mice receiving the same dose intensity (9 mg/kg/week, 27 mg/m²/week) at different dosing schedules are presented in Figure 6. All three schedules delayed tumor growth considerably. However, the two dosing schedules with larger doses given less frequently (9 mg/kg q1wk x 2 or 18 mg/kg) appeared to delay tumor growth to a greater extent than smaller doses given more frequently. When this experiment was repeated, 5 mice had to be euthanized due to toxicity in the group receiving 18 mg/kg. A gross postmortem examination by the University of Alberta's Health Sciences Laboratory staff veterinary pathologist found evidence of cardiac toxicity. This dose is well below the reported LD₅₀ of 38 mg/kg reported for a bolus injection of SL-DXR in CD-1 mice (Working and Dayan, 1996). Whether this difference was because of strain-specific differences in sensitivity to doxorubicin or was tumor-related was not examined further. No further experiments were carried out with this dose.

DISCUSSION

The results from these murine experiments suggest that this species is a reasonable animal model for studying factors influencing the development of Doxil[®]-associated PPE. We demonstrated that repeat administration of SL-DXR using short dose intervals (q1wk) resulted in an accumulation of doxorubicin in the cutaneous tissues of mice. Multiple doses were shown to increase the incidence of mice developing PPE-like lesions. We also demonstrated that lengthening the dose interval allows for more accumulated drug to be cleared from these tissues, resulting in fewer PPE-like lesions in mice. These experimental results confirm clinical observations that longer dose intervals in humans reduced the incidence and severity of PPE (Uziely et al., 1995; Ranson et al., 1997). If our murine results can be extrapolated to humans, then dose delay appears to be useful in controlling PPE because it allows time for drug to be cleared from the skin and for existing lesions to heal. However, as shown here, the advantages of dose delay may be offset by reduced therapeutic activity.

A recent review of toxicities associated with Doxil[®] in patients with metastatic breast cancer provides support for our model (Lyass et al., 2000). The recommended dose intensity for these patients was ~12 mg/m²/week (e.g. 40-50 mg/m² q4wk) and the average plasma t_{1/2} was 79.4 hours, corresponding to 8.5 times the plasma t_{1/2} for SL-DXR administered every 4 weeks. Our data mimic these clinical data in that a dose interval of q2wk (13.5 mg/m²/week) corresponds to 8.5 plasma t_{1/2} (the average plasma t_{1/2} in naïve mice was 39.4 hours). Interestingly, our experiments show that a dose of 13.5 mg/m²/wk resulted in good therapeutic efficacy, combined with low levels of PPE-like symptoms.

It is also important to note that the plasma $t_{1/2}$ did not change substantially for multiple doses of SL-DXR, although there was a modest increase in $t_{1/2}$ after the first dose for each schedule. This is significant because the development of PPE has been correlated to the plasma half-life of SL-DXR (Lyass et al., 2000). If SL-DXR is cytotoxic to cells of the mononuclear phagocyte system (MPS), which is responsible for clearing liposomes, then multiple dose regimes could result in extended $t_{1/2}$ as a result of impaired clearance mechanisms (Daemen et al., 1995). We conclude that the dose schedules used in this study did not impair MPS function to a degree that affected the pharmacokinetics of SL-DXR. This lack of substantial MPS toxicity with SL-DXR is consistent with studies from other laboratories (Storm et al., 1998).

The observation that skin and paw pharmacokinetic parameters were different from those for plasma is interesting. Plasma drug levels fell to low values between doses for even a q1wk dose schedule, while skin and paws drug levels remained elevated for several days. Plasma levels in mice have been important for determining the dosing schedule for liposomal drugs in efficacy studies, and a q1wk schedule is often chosen. This schedule is based on clearance of inert liposomal markers such as ^{125}I -tyraminylinulin in naïve mice ($t_{1/2}$ of 18–24 h in liposomes of similar composition to those used in these studies) (Allen et al., 1993). Hence within 1 week (>8 half-lives) this marker would be cleared almost completely from the plasma of mice. However, the clearance rate of doxorubicin is approximately 2-fold longer than the clearance rate of ^{125}I -tyraminylinulin (an average 39 h in naive mice) and 8 half-lives, in this case, corresponds to one dose every 2 weeks. The difference between the $t_{1/2}$ of doxorubicin and ^{125}I -tyraminylinulin liposomes reflects differences in release rates and volumes of

distribution of the two compounds. Further, loading doxorubicin into liposomes has been shown to increase their circulation times in other models (Bally et al., 1989). Regardless of the model, these data demonstrate that pharmacokinetic studies that do not follow the pharmacologically active agent should be interpreted with caution.

The half-life of SL-DXR was shorter in tumor-bearing mice than in naïve mice. This is consistent with work by Hong et al., who found that the $t_{1/2}$ for SL-DXR was shorter in mice bearing subcutaneous implants of the C26 colon carcinoma (19.1 hours) than in naïve mice (25.1 hours) (Hong et al., 1999). This can partially be explained by significant distribution of drug-loaded liposomes to tumors.

Our results show that half-lives for elimination of drug from skin, paws, and tumors were longer than that for plasma. A longer $t_{1/2}$ will lead to retention of drug in tumors and, arguably, improved antitumor effects, but longer $t_{1/2}$ values in cutaneous tissues will lead to unwanted side effects such as PPE. The challenge is to find the proper balance between minimizing PPE and maintaining therapeutic activity. Our studies show that increasing the dose interval to q2wk did not significantly affect the therapeutic outcome in our tumor model; however, extending the dose interval to q4wk compromised the therapeutic activity.

Skin concentrations of doxorubicin, and their respective AUCs, continued to increase with each successive dose (Table 1). This may be a consequence of skin cytotoxicity accompanied by inflammation. It is well known that inflamed tissue, like tumor tissue, has increased capillary permeability and can accumulate liposomes via the enhanced permeability and retention (EPR) effect (Matsumura and Maeda, 1986; Maeda et al., 2000). This will increase localization of liposomes into skin with subsequent

injections in a vicious cycle. Alternatively, since our dorsal skin samples were not subject to pressure or irritation, the increased localization of liposomes into skin may reflect an increase to steady-state levels, which normally occurs within 3 to 5 doses. For drug clearance, an interval of 5 half-lives results in approximately 3% of the total dose remaining in tissues. For skin, 5 half-lives would be approximately 23 days, roughly corresponding to the q4wk dosing interval that produced the lowest incidence of PPE-like lesions.

One unexpected observation was the decrease in the C_{\max} for paws using the q2wk and q4wk dose schedules. This decrease was not due to the alterations in the plasma pharmacokinetics (i.e., $t_{1/2}$ values did not decrease). Therefore, fewer liposomes localized in paws. This may be a result of doxorubicin-associated tissue damage causing tissue remodeling or scarring, which would reduce the ability of subsequent doses to accumulate. Alternatively, it could be due to a reduction in the pressure-dependent extravasation of liposomes if mice developed “sore paws” (PPE-like lesions) and moved around their cages less, although this was not specifically measured.

The cytotoxicity of doxorubicin is not cell cycle-dependent; therefore, one can speculate that the antitumor activity of doxorubicin might be dependent upon tumor C_{\max} . Our therapeutic studies demonstrated that SL-DXR doses of 9 mg/kg q1wk or 18 mg/kg doxorubicin, which result in higher peak concentrations of total drug, had better therapeutic activity than smaller doses (4.5 mg/kg) given more frequently.

As previously observed (Charrois and Allen, 2003), and as verified in these experiments, the 4T1 tumor accumulates liposomes at a faster rate than either skin or paws. Therefore, it may be possible to reduce the incidence of SL-DXR-associated

cutaneous toxicities by engineering a liposomal drug delivery system, e.g., a triggered release system, that accumulates in tumors, and releases its contents prior to maximal liposome accumulation in skin or paws. This hypothesis is supported by work by Needham et al., who demonstrated improved therapeutic outcomes in tumor-bearing mice when doxorubicin release was triggered by hyperthermia in single tumors (i.e., not metastatic disease) (Needham et al., 2000).

Our study measured total doxorubicin, which includes both liposome-encapsulated and released drug. An important consideration in pharmacokinetic, biodistribution, and therapeutic studies with liposomes is the bioavailability of the drug. As long as the drug, e.g., doxorubicin, remains encapsulated within the liposomes, it is not bioavailable and will have no biological activity, including no antitumor effect. It is possible to have high tissue AUCs for liposomal drugs, but low levels of efficacy, if the drug is released very slowly, since minimal therapeutic levels of drug in tissues may not be reached. At the opposite end of the spectrum, if the drug is released too rapidly, before the liposomes localize in target tissues, the therapeutic effects may not be different from the administration of nonencapsulated drug. In order to determine optimum drug release rates, it will be necessary to develop methods for measuring bioavailable drug in the target tissues and in the tissues that are subject to toxic side effects; this has been a relatively neglected area of liposome research (Krishna et al., 2001). However, several laboratories are developing methods to trigger the release of liposomal contents once the liposomes have accumulated in target tissues such as tumors (Adlakha-Hutcheon et al., 1999; Kong et al., 2000; Goldberg et al., 2002).

In summary, these studies using a murine model reinforce the importance of dose schedule and dose intensity on the therapeutic activity and cutaneous toxicity of SL-DXR, and provide the first experimental data on the pharmacokinetics and biodistribution of liposomal doxorubicin in tumor and cutaneous tissue for multiple dosing schedules. They also provide experimental evidence supporting the utility of a mouse model for predicting side effects and therapeutic activity in the clinic.

Acknowledgments

The authors gratefully acknowledge Dr. Dion Brocks (Faculty of Pharmacy, University of Alberta) for helpful discussions. The technical assistance for tumor implantation of Elaine Moase, Janny Zhang, and the University of Alberta Health Sciences Laboratory Animal Services is also gratefully acknowledged, as well as Dr. Richard Uwiera for performing gross pathological examinations.

References

Adlakha-Hutcheon G, Bally MB, Shew CR and Madden TD (1999) Controlled destabilization of a liposomal drug delivery system enhances mitoxantrone antitumor activity. *Nat Biotechnol* 17:775-779.

Allen TM and Hansen CB (1991) Pharmacokinetics of Stealth versus conventional liposomes: effect of dose. *Biochim Biophys Acta* 1068:133-141.

Allen TM, Hansen CB and Guo LSS (1993) Subcutaneous administration of liposomes: a comparison with the intravenous and intraperitoneal routes of injection. *Biochim Biophys Acta* 1150:9-16.

Allen TM, Hansen CB and Lopes de Menezes DE (1995) Pharmacokinetics of long circulating liposomes. *Adv Drug Delivery Rev* 16:267-284.

Allen TM, Hansen CB, Martin F, Redemann C and Yau-Young A (1991) Liposomes containing synthetic lipid derivatives of poly(ethylene glycol) show prolonged circulation half-lives in vivo. *Biochim Biophys Acta* 1066:29-36.

Amantea M, Newman MS, Sullivan TM, Forrest A and Working PK (1999) Relationship of dose intensity to the induction of palmar-plantar erythrodysesthesia by pegylated liposomal doxorubicin in dogs. *Hum Exp Toxicol* 18:17-26.

Aslakson CJ and Miller FR (1992) Selective events in the metastatic process defined by analysis of the sequential dissemination of subpopulations of a mouse mammary tumor. *Cancer Res* 52:1399-1405.

Bally MB, Nayar R, Masin D, Hope MJ, Cullis PR and Mayer LD (1989) Liposomes with entrapped doxorubicin exhibit extended blood residence times. *Biochim Biophys Acta* 1023:133-139.

Berry G, Billingham M, Alderman E, Richardson P, Torti F, Lum B, Patek A and Martin FJ (1998) The use of cardiac biopsy to demonstrate reduced cardiotoxicity in AIDS Kaposi's sarcoma patients treated with pegylated liposomal doxorubicin. *Ann Oncol* 9:711-716.

Charrois GJR and Allen TM (2003) Rate of biodistribution of STEALTH[®] liposomes to tumor and skin: influence of liposome diameter and implications for toxicity and therapeutic activity. *Biochim Biophys Acta* 1609:102-108.

Cowens JW, Creaven PJ, Greco WR, Brenner DE, Tung Y, Osto M, Pilkiewicz F, Ginsberg R and Petrelli N (1993) Initial clinical (phase I) trial of TLC D-99 (doxorubicin encapsulated in liposomes). *Cancer Res* 53:2796-2802.

Daemen T, Hofstede G, Ten Kate MT, Bakker-Woudenberg IA and Scherphof GL (1995) Liposomal doxorubicin-induced toxicity: depletion and impairment of phagocytic activity of liver macrophages. *Int J Cancer* 61:716-721.

Freireich EJ, Gehan EA, Rall DP, Schmidt LH and Skipper HE (1966) Quantitative comparison of toxicity of anticancer agents in mouse, rat, hamster, dog, monkey and man. *Cancer Chemother Rep* 50:219-244.

Gabizon A (2001) Stealth liposomal doxorubicin: An analysis of the effect of dose on tumor targeting and therapy, in *Fifth International Conference: Liposome Advances: progress in drug and vaccine delivery* (G. Gregoriadis and A.T. Florence, editors).

Gabizon A, Catane R, Uziely B, Kaufman B, Safra T, Cohen R, Martin F, Huang A and Barenholz Y (1994a) Prolonged circulation time and enhanced accumulation in malignant exudates of doxorubicin encapsulated in polyethylene-glycol coated liposomes. *Cancer Res* 54:987-992.

Gabizon A, Isacson R, Libson E, Kaufman B, Uziely B, Catane R, Ben-Dor CG, Rabello E, Cass Y, Peretz T, Sulkes A, Chisin R and Barenholz Y (1994b) Clinical studies of liposome-encapsulated doxorubicin. *Acta Oncol* 33:779-786.

Goldberg SN, Kamel IR, Kruskal JB, Reynolds K, Monsky WL, Stuart KE, Ahmed M and Raptopoulos V (2002) Radiofrequency ablation of hepatic tumor: increased tumor destruction with adjuvant liposomal doxorubicin therapy. *Am J Roentgenol* 179:93-101.

Gordon AN, Granai CO, Rose PG, Hainsworth J, Lopez A, Weissman C, Rosales R and Sharpington T (2000) Phase II study of liposomal doxorubicin in platinum- and paclitaxel-refractory epithelial ovarian cancer. *J Clin Oncol* 18:3093-3100.

Gordon KB, Tajuddin A, Guitart J, Kuzel TM, Eramo LR and VonRoenn J (1995) Hand-foot syndrome associated with liposome-encapsulated doxorubicin therapy. *Cancer* 75:2169-2173.

Hamilton A, Biganzoli L, Coleman R, Mauriac L, Hennebert P, Awada A, Nooij M, Beex L, Piccart M, Van Hoorebeeck I, Bruning P and de Valeriola D (2002) EORTC 10968: a phase I clinical and pharmacokinetic study of polyethylene glycol liposomal doxorubicin (Caelyx[®], Doxil[®]) at a 6-week interval in patients with metastatic breast cancer. *Ann Oncol* 13:910-918.

Hensley ML, Hoppe B, Leon L, Sabbatini P, Aghajanian C, Chi D and Spriggs DR (2001) The costs and efficacy of liposomal doxorubicin in platinum-refractory ovarian cancer in heavily pretreated patients. *Gynecol Oncol* 82:464-469.

Hong R-L, Huang C-J, Tseng Y-L, Pang VF, Chen S-T, Liu J-J and Chang F-H (1999) Direct comparison of liposomal doxorubicin with or without polyethylene glycol coating in C-26 tumor-bearing mice: Is surface coating with polyethylene glycol beneficial? *Clin Cancer Res* 5:3645-3652.

Kong G, Anyarambhatla G, Petros WP, Braun RD, Colvin OM, Needham D and Dewhirst MW (2000) Efficacy of liposomes and hyperthermia in a human tumor xenograft model: importance of triggered drug release. *Cancer Res* 60:6950-6957.

Krishna R, Ghiu G and Mayer LD (2001) Visualization of bioavailable liposomal doxorubicin using a non-perturbing confocal imaging technique. *Histol Histopathol* 16:693-699.

Lotem M, Hubert A, Lyass O, Goldenhersh MA, Ingber A, Peretz T and Gabizon A (2000) Skin toxic effects of polyethylene glycol-coated liposomal doxorubicin. *Arch Dermatol* 136:1474-1480.

Lyass O, Uziely B, Ben-Yosef R, Tzemach D, Heshing NI, Lotem M, Brufman G and Gabizon A (2000) Correlation of toxicity with pharmacokinetics of pegylated liposomal doxorubicin (Doxil) in metastatic breast carcinoma. *Cancer* 89:1037-1047.

Maeda H, Wu J, Sawa T, Matsumura Y and Hori K (2000) Tumor vascular permeability and the ERP effect in macromolecular therapeutics: a review. *J Control Release* 65:271-284.

Matsumura Y and Maeda H (1986) A new concept for macromolecular therapeutics in cancer chemotherapy; mechanism of tumoritropic accumulation of proteins and the antitumor agent SMANCS. *Cancer Res* 6:6387-6392.

Mayer LD, Dougherty G, Harasym TO and Bally MB (1997) The role of tumor-associated macrophages in the delivery of liposomal doxorubicin to solid murine fibrosarcoma tumors. *J Pharmacol Exp Ther* 280:1406-1414.

Moase E, Qi W, Ishida T, Gabos Z, Longenecker BM, Zimmermann GL, Ding L, Krantz M and Allen TM (2001) Anti-MUC-1 immunoliposomal doxorubicin in the treatment of murine models of metastatic breast cancer. *Biochim Biophys Acta* 1510:43-55.

Muggia F, Hainsworth JD, Jeffers S, Miller P, Groshen S, Tan M, Roman L, Uziely B, Muderspach L, Garcia A, Burnett A, Greco FA, Morrow CP, Paradiso LJ and Liang L-J (1997) Phase II study of liposomal doxorubicin in refractory ovarian cancer: antitumor activity and toxicity modification by liposomal encapsulation. *J Clin Oncol* 15:987-993.

Needham D, Anyarambhatla G, Kong G and Dewhirst MW (2000) A new temperature-sensitive liposome for use with mild hyperthermia: characterization and testing in a human tumour xenograft model. *Cancer Res* 60:1197-1201.

Northfelt DW, Dezube BJ, Thommes JA, Levine R, Von Roenn JH, Dosik GM, Rios A, Krown SE, DuMond C and Mamelok RD (1997) Efficacy of pegylated-liposomal doxorubicin in the treatment of AIDS-related Kaposi's sarcoma after failure of standard chemotherapy. *J Clin Oncol* 15:653-659.

Papahadjopoulos D, Allen TM, Gabizon A, Mayhew E, Matthay K, Huang SK, Lee KD, Woodle MC, Lasic DD, Redemann C and Martin FJ (1991) Sterically stabilized liposomes: improvements in pharmacokinetics and antitumor therapeutic efficacy. *Proc Natl Acad Sci U S A* 88:11460-11464.

Ranson MR, Carmichael J, O'Byrne K, Stewart S, Smith D and Howell A (1997) Treatment of advanced breast cancer with sterically stabilized liposomal doxorubicin: results of a multicenter phase II trial. *J Clin Oncol* 15:3185-3191.

Safra T, Muggia F, Jeffers S, Tsao-Wei DD, Groshen S, Lyass O, Henderson R, Berry G and Gabizon A (2000) Pegylated liposomal doxorubicin (Doxil): reduced clinical cardiotoxicity in patients reaching or exceeding cumulative doses of 500 mg/m². *Ann Oncol* 11:1029-1033.

Storm G, ten Kate MT, Working PK and Bakker-Woudenberg IAJM (1998) Doxorubicin entrapped in sterically stabilized liposomes: effects on bacterial blood clearance of the mononuclear phagocyte system. *Clin Cancer Res* 3:111-115.

Uziely B, Jeffers S, Isacson R, Kutsch K, Wei-Tsao D, Yehoshua Z, Libson E, Muggia FM and Gabizon A (1995) Liposomal doxorubicin: antitumor activity and unique toxicities during two complementary phase I studies. *J Clin Oncol* 13:1777-1785.

Working P and Dayan AD (1996) Pharmacological-toxicological expert report: Caelyx[®] (Stealth[®] liposomal doxorubicin HCl). *Hum Exp Toxicol* 15:751-785.

Footnotes

* This research was supported by the Canadian Institutes of Health Research (UOP 48092) and ALZA Corporation (Mountain View, CA). Gregory Charrois is the recipient of a graduate studentship from the Alberta Heritage Foundation for Medical Research.

Reprint requests to: Dr. Terry Allen

Department of Pharmacology

University of Alberta

9-31 Medical Sciences Building

Edmonton, AB Canada T6G 2H7

Figure Legends

Figure 1. Tissue concentrations of doxorubicin in mice given SL-DXR at a dose schedule of 9 mg/kg q1wk. Mice were injected i.v. via the lateral tail vein at weekly intervals (arrows). Data represent the mean \pm S.D. of triplicate aliquots from 4 to 5 mice and are reported as doxorubicin μ equivalents. A) plasma, B) skin, C) paws.

Figure 2. Tissue concentrations of doxorubicin in mice given SL-DXR at a dose schedule of 9 mg/kg q2wk. Details as in Figure 1.

Figure 3. Tissue concentrations of doxorubicin in mice given SL-DXR at a dose schedule of 9 mg/kg q4wk. Details as in Figure 1.

Figure 4. Tissue concentrations of doxorubicin in mice given SL-DXR at the same dose intensity. The BALB/c mice were implanted in the #4 mammary fat pad with the 4T1 tumor and injected i.v. with SL-DXR 10 days later. Data represent the mean \pm S.D. of triplicate aliquots from 5 mice and are expressed as doxorubicin μ equivalents. (A) plasma, (B) tumor, (C) skin, (D) paws. (■) 18 mg/kg q2wk (1 dose), (▲) 9 mg/kg q1wk (2 doses), (●) 4.5 mg/kg q3d (4 doses).

Figure 5. Therapeutic activity of SL-DXR against the 4T1 murine mammary carcinoma using different dose schedules. The BALB/c mice were implanted in the #4 mammary fat pad with the 4T1 murine mammary carcinoma. Four days later mice began i.v. treatment with SL-DXR at a doxorubicin dose of 9 mg/kg with one of three dose schedules: (A) q1wk, (B) q2wk, or (C) q4wk. Control mice received sterile D5W: (▲) control, (●) SL-DXR. Arrows indicate treatment days. Data represent the mean \pm S.D. from 5 to 10 mice.

Figure 6. Therapeutic activity of SL-DXR against the 4T1 murine mammary carcinoma using dose schedules with the same dose intensity. The BALB/c mice were implanted in the #4 mammary fat pad with the 4T1 murine mammary carcinoma. Four days later mice were treated i.v. with SL-DXR at a total drug dose of 18 mg/kg with one of three dose schedules: (A) 4.5 mg/kg q3days, (B) 9 mg/kg q1wk, or (C) 18 mg/kg q2wk. Control mice received sterile D5W: (▲) control, (●) SL-DXR. Arrows indicate treatment days. Data represent the mean \pm S.D. from 5 to 10 mice, except for 18 mg/kg SL-DXR, where n=4 to 5.

Table 1. Pharmacokinetic parameters for mice receiving i.v. SL-DXR at a dose of 9 mg/kg q1wk, q2wk, or q4wk. The AUC values were calculated using the trapezoidal rule. Plasma and tissue $t_{1/2}$ values were calculated using the formula $t_{1/2}=0.693/k_{elm}$, where k_{elm} is the elimination constant derived from the plasma or tissue concentration versus time curve. **(A)** 9 mg/kg q1wk. **(B)** 9 mg/kg q2wk. **(C)** 9 mg/kg q4wk.

A.

Dose	Plasma		Skin		Paws	
	$t_{1/2}^a$	AUC ^b	$t_{1/2}^a$	AUC ^c	$t_{1/2}^a$	AUC ^c
1	39.4	9141	ND	589	ND	1473
2	43.0	14648	ND	1010	ND	1446
3	43.0	12628	ND	1680	ND	1549
4	44.7	12249	ND	1592	ND	1475
C_{ss}	n/a	72.9	n/a	9.48	n/a	8.78

B.

Dose	Plasma		Skin		Paws	
	$t_{1/2}^a$	AUC ^b	$t_{1/2}^a$	AUC ^c	$t_{1/2}^a$	AUC ^c
1	28.6	9267	58.2	865	81.5	2308
2	35.2	12359	37.9	1283	100	2071
3	41.5	12450	139	1792	157	1454
4	44.4	12302	218	1964	178	1384
C_{ss}	n/a	33.2	n/a	5.84	n/a	4.11

C.

Dose	Plasma		Skin		Paws	
	$t_{1/2}^a$	AUC ^b	$t_{1/2}^a$	AUC ^c	$t_{1/2}^a$	AUC ^c
1	41.5	9813	136	800	103	3213
2	33.2	9962	103	1136	147	1717
3	31.6	11019	147	1337	198	1465
4	46.8	10727	105	1595	192	1645
C_{ss}	n/a	14.6	n/a	2.37	n/a	2.45

ND = not determined

^a $t_{1/2}$ (hours)

^b Units for plasma AUC are doxorubicin μ equivalents x h / mL.

^c Units for skin and paw AUCs are doxorubicin μ equivalents x h / g.

Table 2. Numbers (percent) of mice developing PPE-like lesions as a function of dose schedule. Values represent the number of mice with PPE-like lesions at the time of receiving the stated dose. For each dose schedule mice were injected i.v. with SL-DXR at a DXR dose of 9 mg/kg.

Dose Schedule	Dose 2	Dose 3	Dose 4
q1wk	0/75 (0 %)	8/50 (16 %)	17/24 (70 %)
q2wk	5/75 (7 %)	5/50 (10 %)	8/25 (32 %)
q4wk	3/90 (3 %)	3/60 (5 %)	0/30 (0 %)

Table 3. Pharmacokinetic parameters for mice receiving SL-DXR at a dose intensity of 9 mg/kg/week. Mice received i.v. either four doses at 4.5 mg/kg q3d, two doses at 9 mg/kg q1wk or one dose at 18 mg/kg. The AUC values were calculated using the trapezoidal rule. Plasma $t_{1/2}$ values were calculated using the formula $t_{1/2}=0.693/k_{elm}$, where k_{elm} is the elimination constant derived from the plasma concentration versus time curve.

Dose schedule	Plasma		Skin	Paws	Tumor
	$t_{1/2}$	AUC ^a	AUC ^b	AUC ^b	AUC ^b
4.5 mg/kg q3d					
Dose 1 AUC _(0-72h)	34.6	2070	125	276	916
Dose 2 AUC _(0-72h)	25.4	4208	133	368	965
Dose 3 AUC _(0-72h)	33.0	4506	162	424	1524
Dose 4 AUC _(0-72h)	29.5	4505	136	382	1965
Total AUC _(0-∞)		15884	963	2737	12214
9 mg/kg q1wk					
Dose 1 AUC _(0-168h)	26.3	6987	451	1235	4844
Dose 2 AUC _(0-168h)	22.2	7520	661	1160	6246
Total AUC _(0-∞)		14539	1512	3145	14612
18 mg/kg q2wk					
Dose 1 AUC _(0-∞)	29.5	17891	1322	3782	14809

^a Units for plasma AUC are doxorubicin μ equivalents x h / mL

^b Units for tumor, skin, and paw AUCs are doxorubicin μ equivalents x h / g

Figure 1

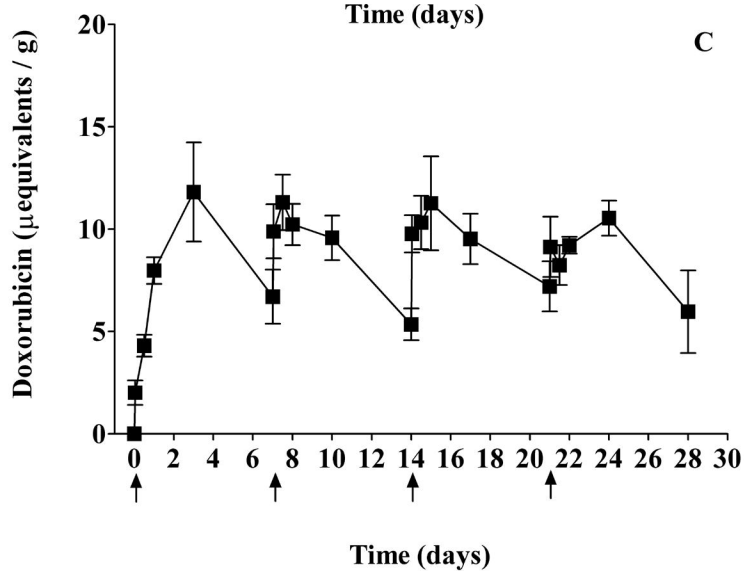
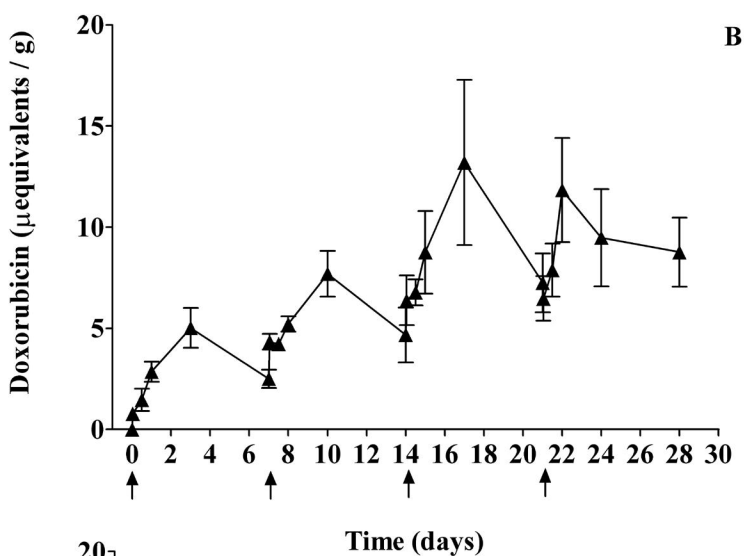
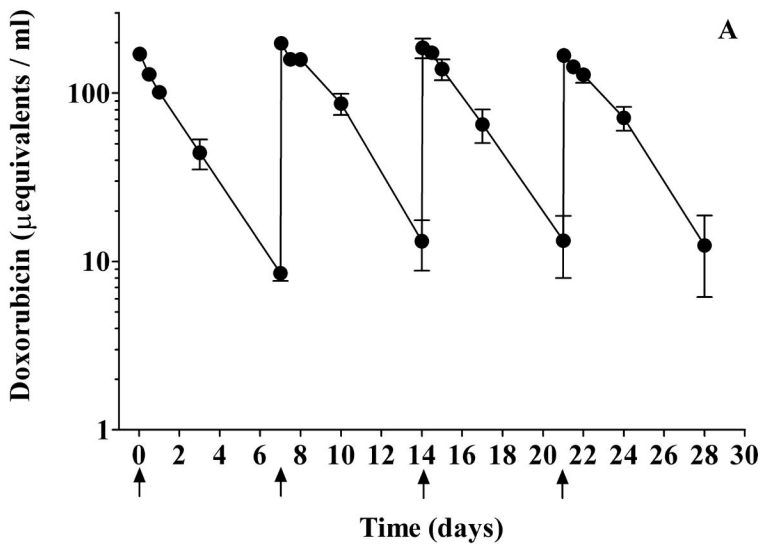


Figure 2

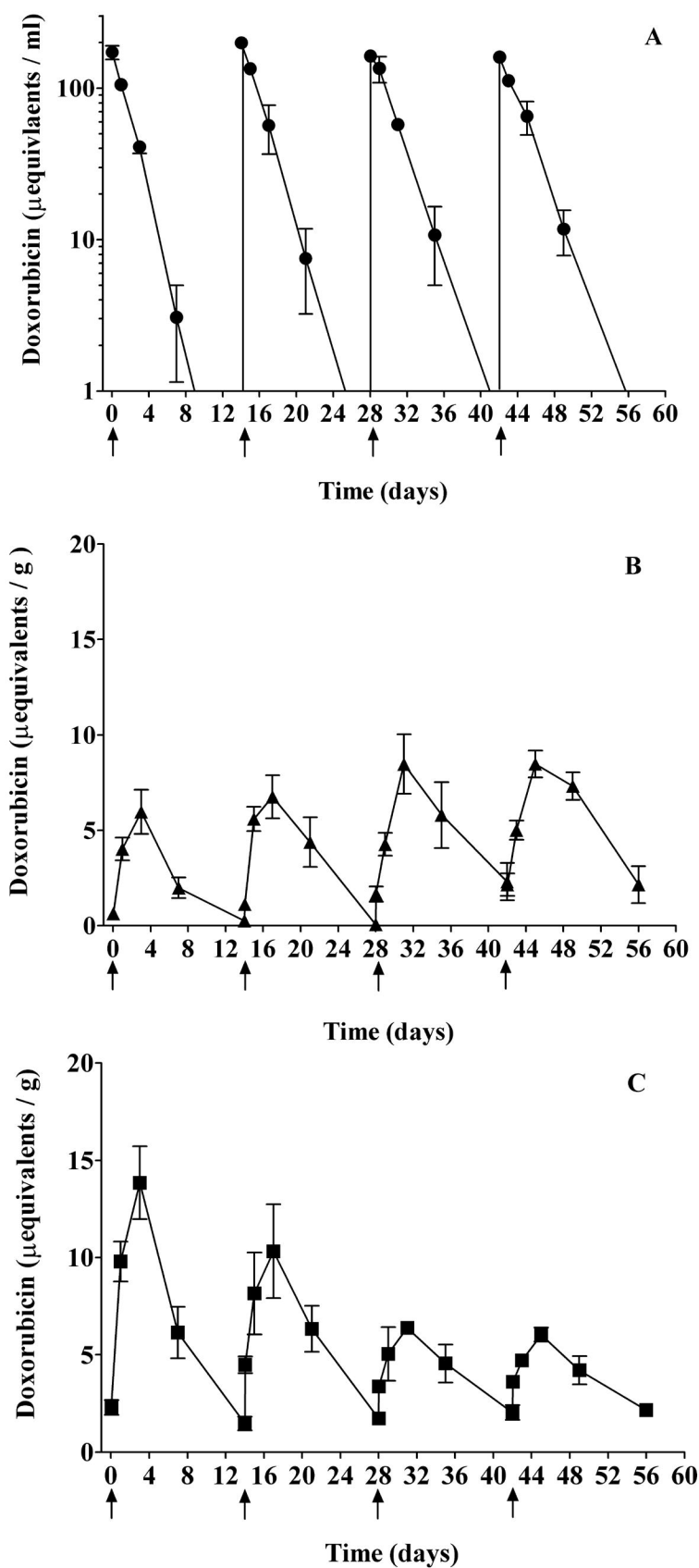


Figure 3

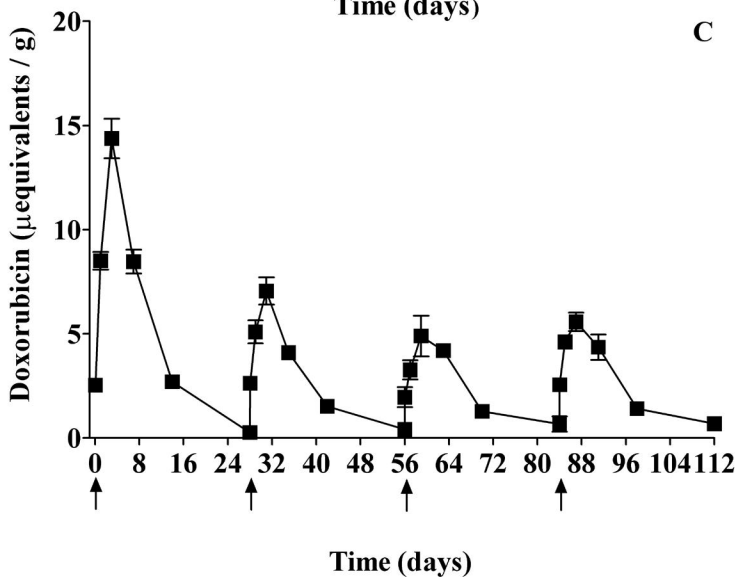
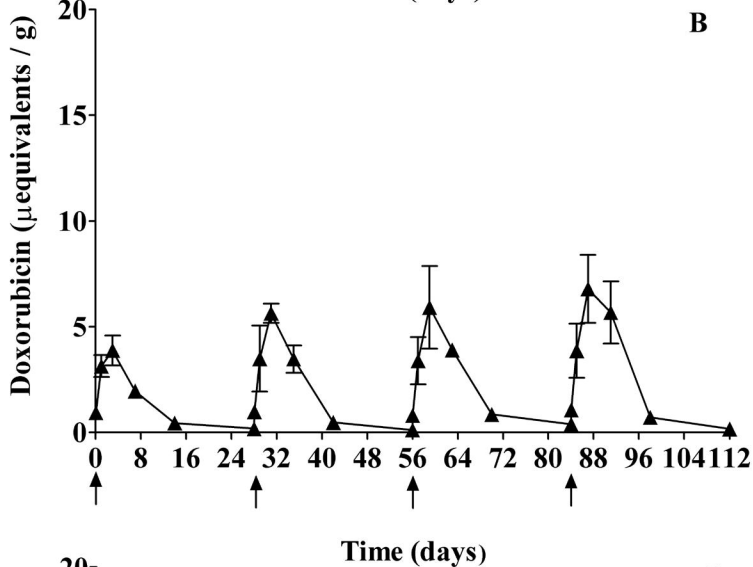
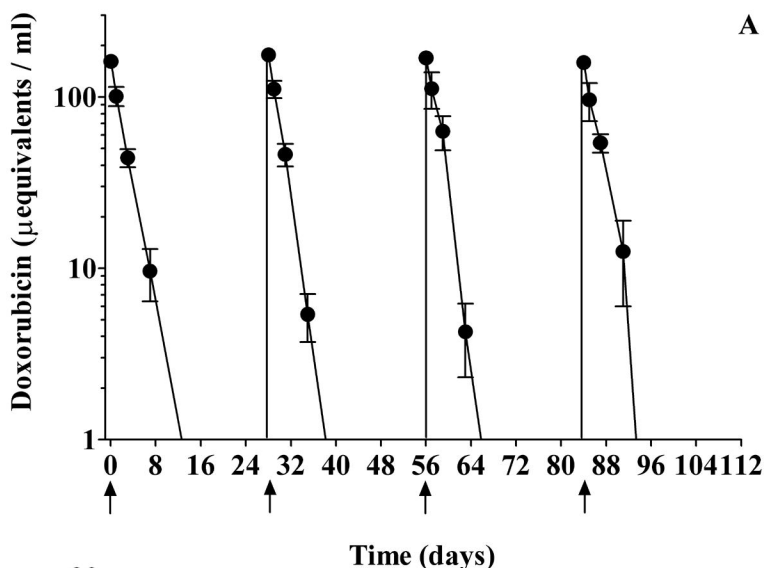


Figure 4

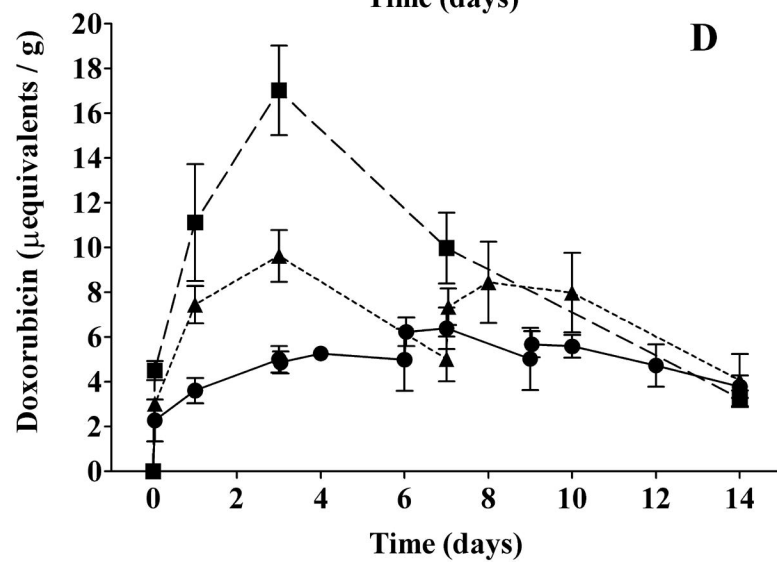
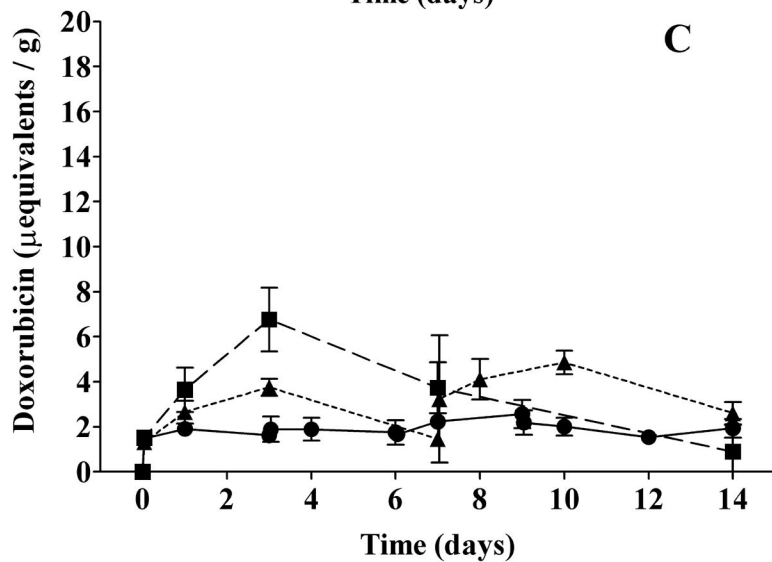
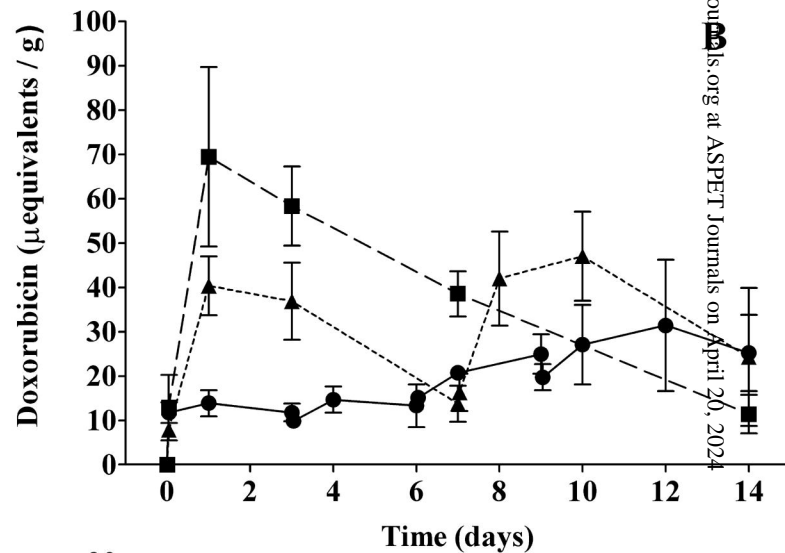
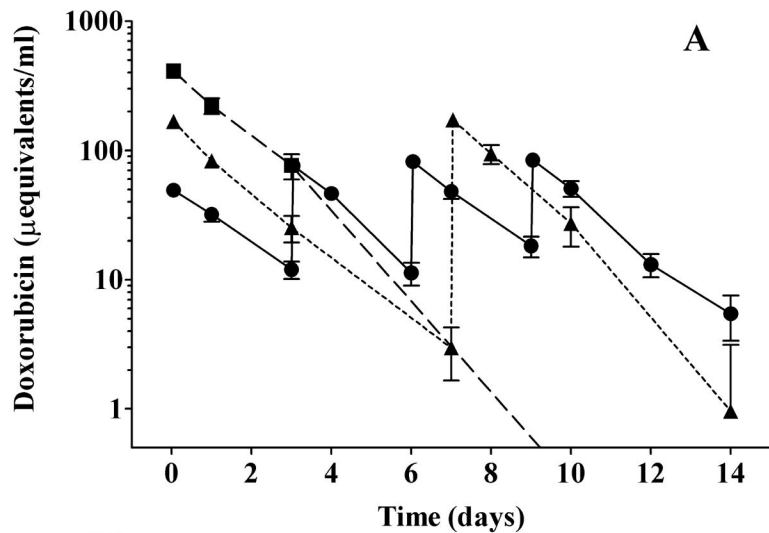


Figure 5

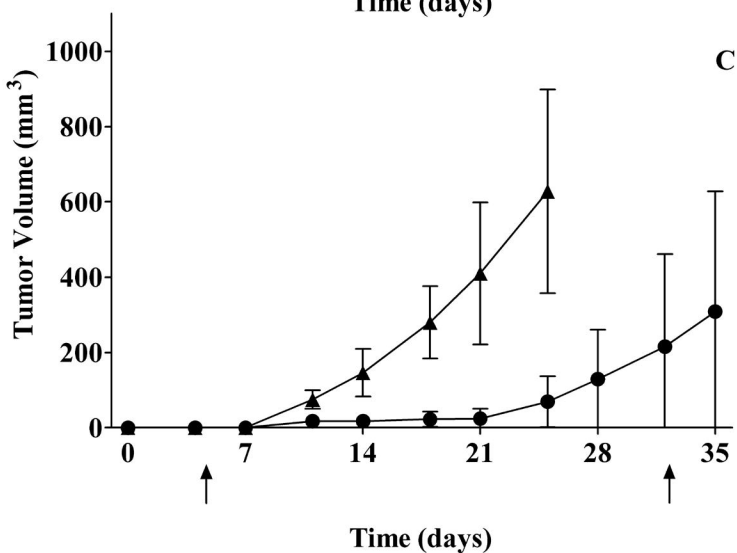
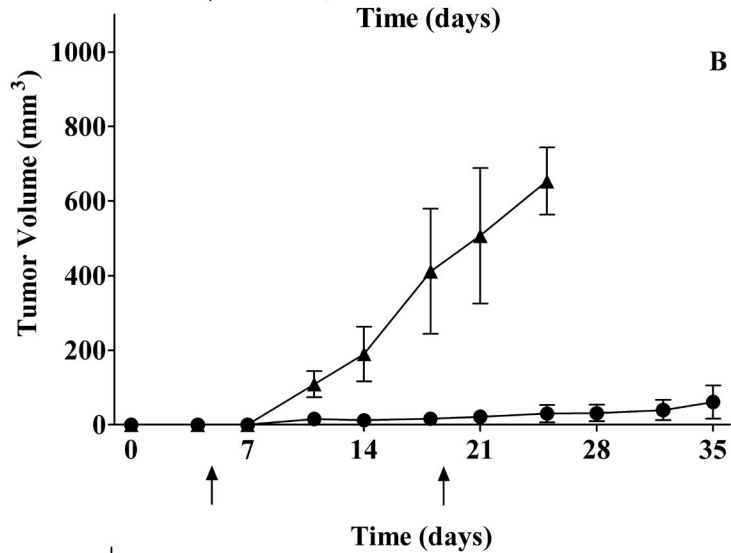
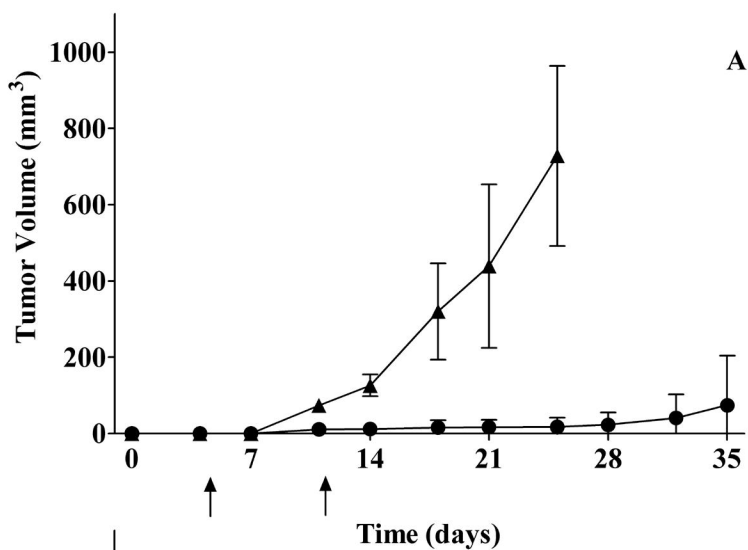


Figure 6

